Supplementary information:

A sub-organ-resolved pan-tissue single-cell atlas reveals cell-type-specific molecular regulation and xenotransplantation potential in pigs

Hong Hu[1,2,6], Xi Bai[1,3,6], Cao Deng[4,5,6], Anjian Li[1,6], Yichao Mei[5], Taozong Guo[1], Yuting Yang[1,2], Shaokan Tang[5], Lei Sun[5], Fei Zhao[5], Xiangfang Zeng[2,*], Shiyan Qiao[2,*], Hongbin Pan[1,*],

[1]Yunnan Provincial Key Laboratory of Animal Nutrition and Feed Science, Faculty of Animal Science and Technology, Yunnan Agricultural University, Kunming, China

[2]State Key Laboratory of Animal Nutrition and Feeding, Ministry of Agriculture and Rural Affairs Feed Industry Center, China Agricultural University, Beijing, China

[3] College of Animal Science, Anhui Science and Technology University, Chuzhou, China

[4]Key Laboratory of Animal Disease and Human Health of Sichuan Province, College of Veterinary Medicine, Sichuan Agricultural University, Chengdu, China

[5]Departments of Bioinformatics, DNA Stories Bioinformatics Center, Chengdu, China

[6]These authors contributed equally: Hong Hu, Xi Bai, Cao Deng, Anjian Li

[*]Correspondence: ziyangzxf@163.com, qiaoshiyan@cau.edu.cn, Pynnydx@163.com

Supplementary Figures

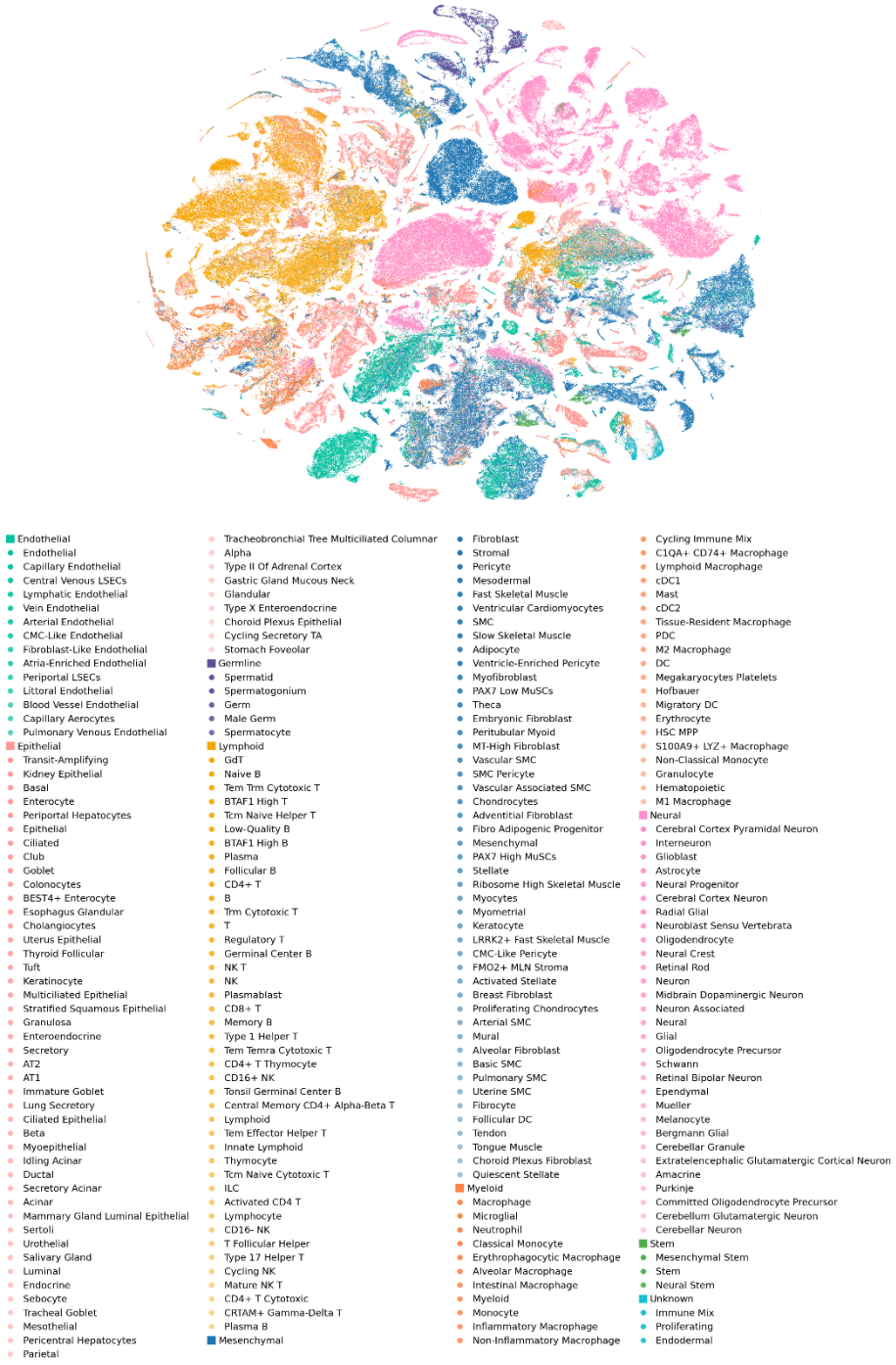

Supplementary Fig. S1 t-SNE plot of porcine single cells colored by 228 cell-type annotations. The clustering diagram classifies and colour codes cells according to 228 clusters. The nine colour schemes in the figure represent nine distinct superclusters (i.e., the nine major categories of cell type annotation). Within each supercluster, different colours denote different clusters, where the numbers in parentheses indicate cell counts.

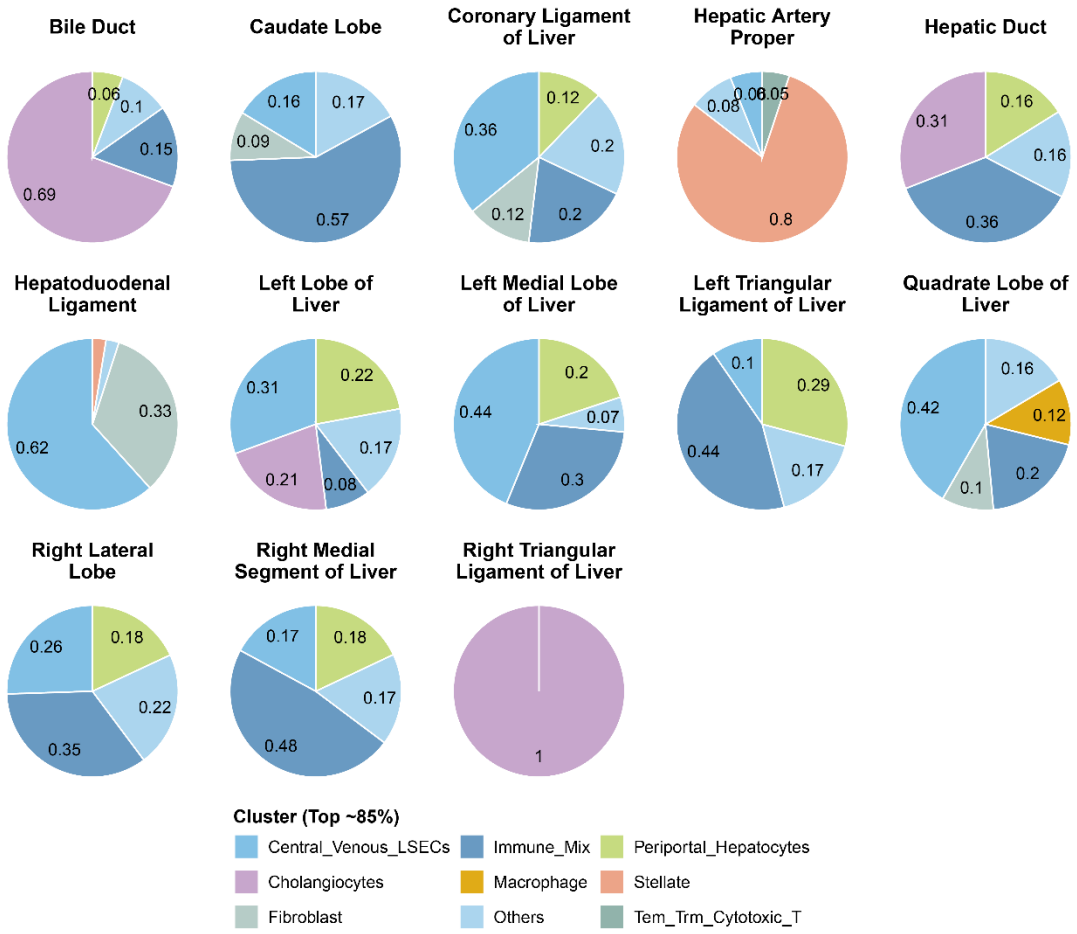

Supplementary Fig. S2 Cell-type composition of different hepatic lobes.

The “Others” group in the pie chart aggregates rare cell types with small cell numbers. Cell types were ranked by cell count in descending order; the top 85% were individually shown, while the remaining 15% were combined as “Others”.

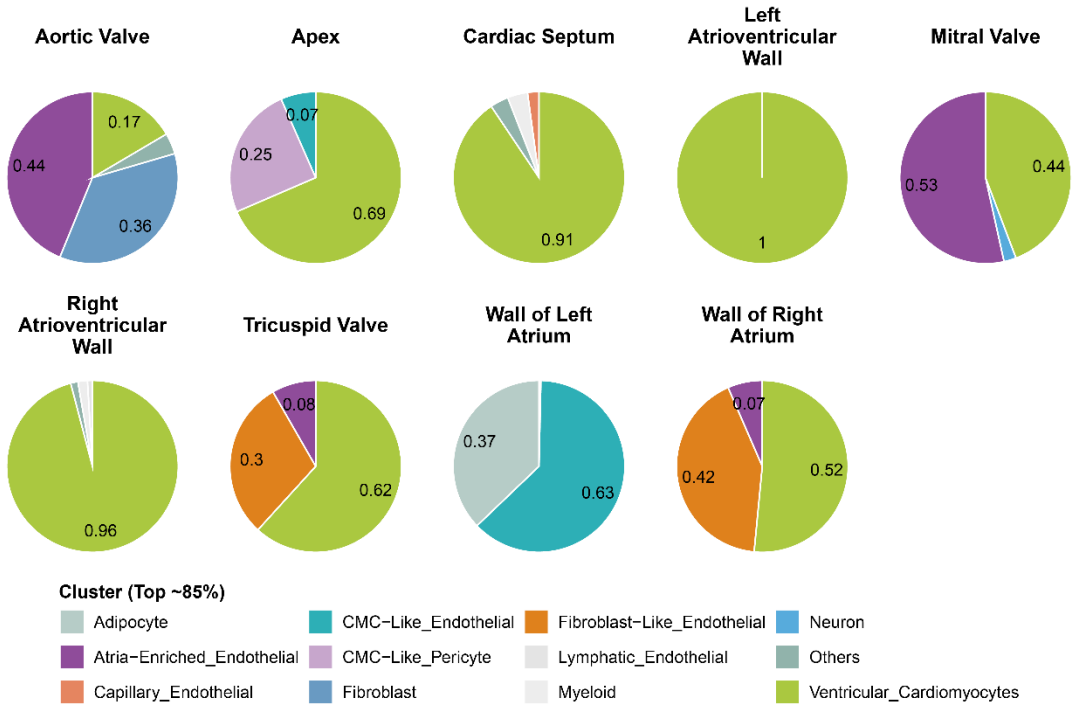

Supplementary Fig. S3 Cell-type composition of cardiac sub-regions.

The “Others” group in the pie chart aggregates rare cell types with small cell numbers. Cell types were ranked by cell abundance in descending order: the top 85% were shown separately, while the remaining 15% were combined as “Others”.

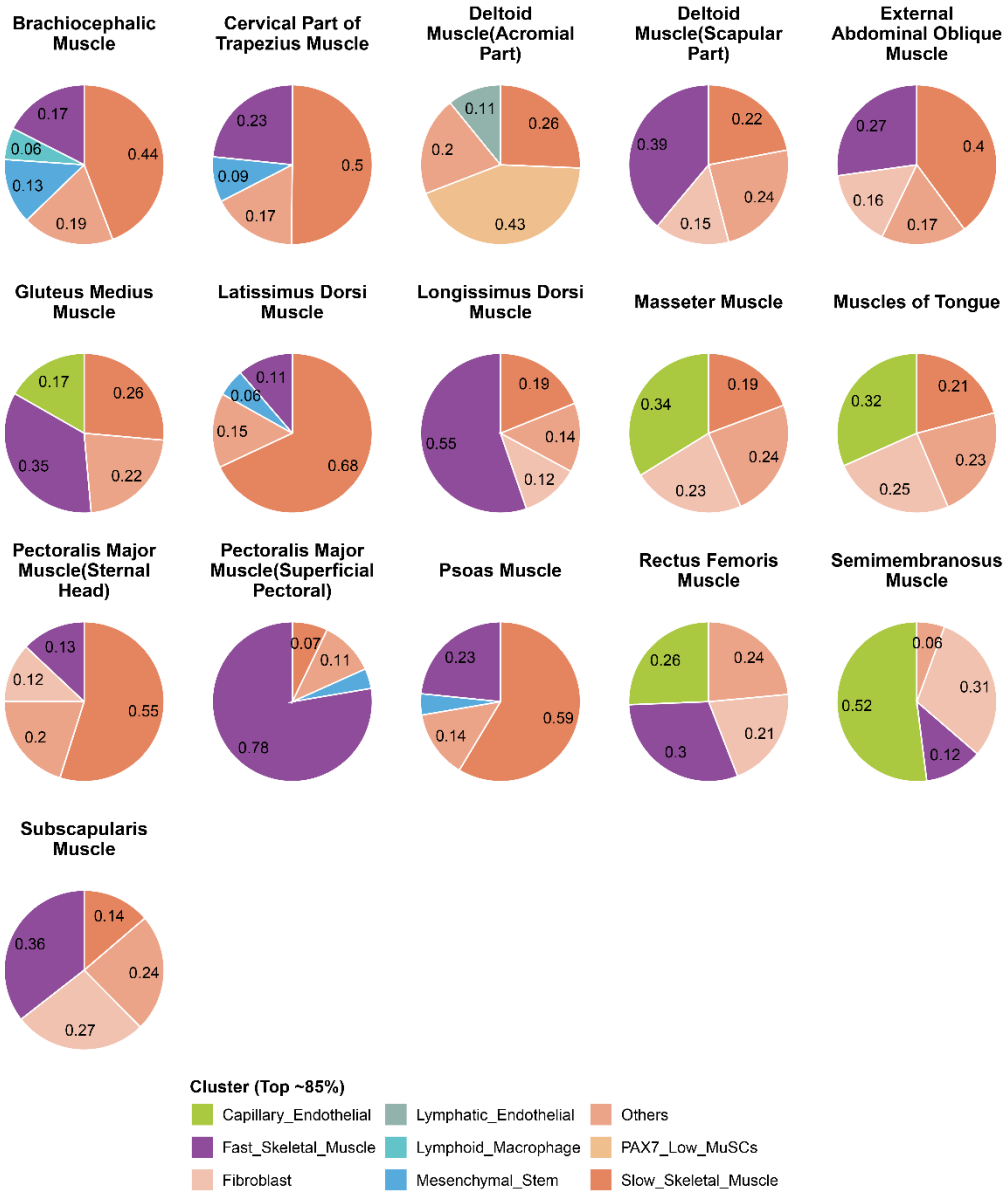

Supplementary Fig. S4 Cell-type composition of sub-regions in skeletal muscle.

The “Others” group in the pie chart aggregates rare cell types with small cell numbers. Cell types were ranked by cell abundance in descending order: the top 85% were shown separately, while the remaining 15% were combined as “Others”.

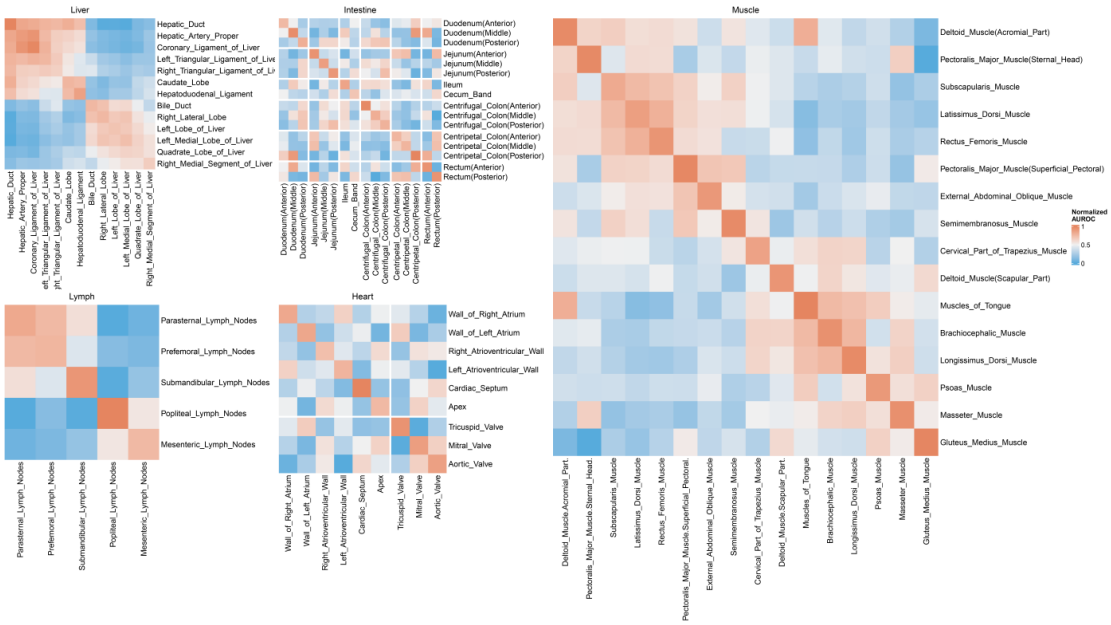

Supplementary Fig. S5 Transcriptional similarity map of suborgans.

This heatmap depicts the transcriptional similarity among suborgans from the liver, intestine, muscle, lymph, and heart. Suborgans are ordered according to their anatomical structure. The colour gradient, from red (high similarity) to blue (low similarity), reflects the homogeneity of functional states across these suborgans.

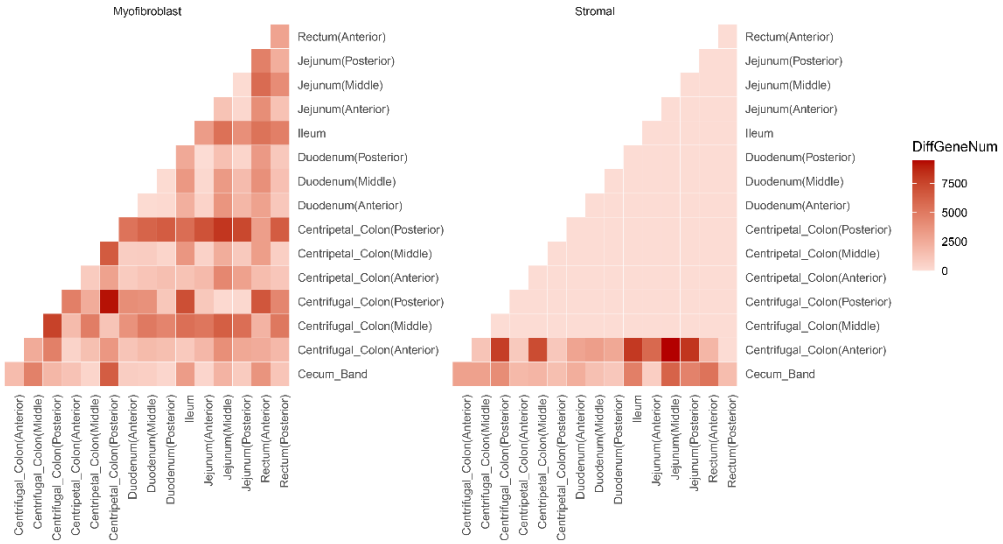

Supplementary Fig. S6 DEG identification among gastrointestinal sub-organs.

Color depth indicates the count of DEGs with adjusted p-value < 0.01 and $|\log_2 \text{foldchange}| > 1$.

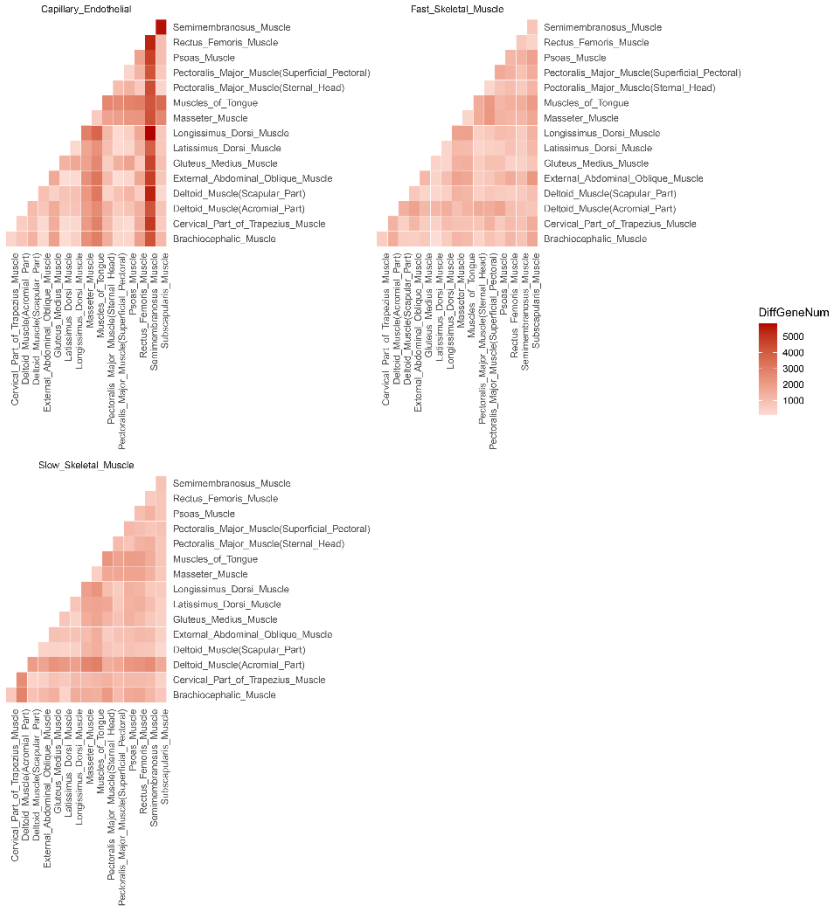

Supplementary Fig. S7 DEG identification among skeletal muscle sub-organs.

Color depth indicates the count of DEGs with adjusted p-value < 0.01 and $|\log_2 \text{foldchange}| > 1$.

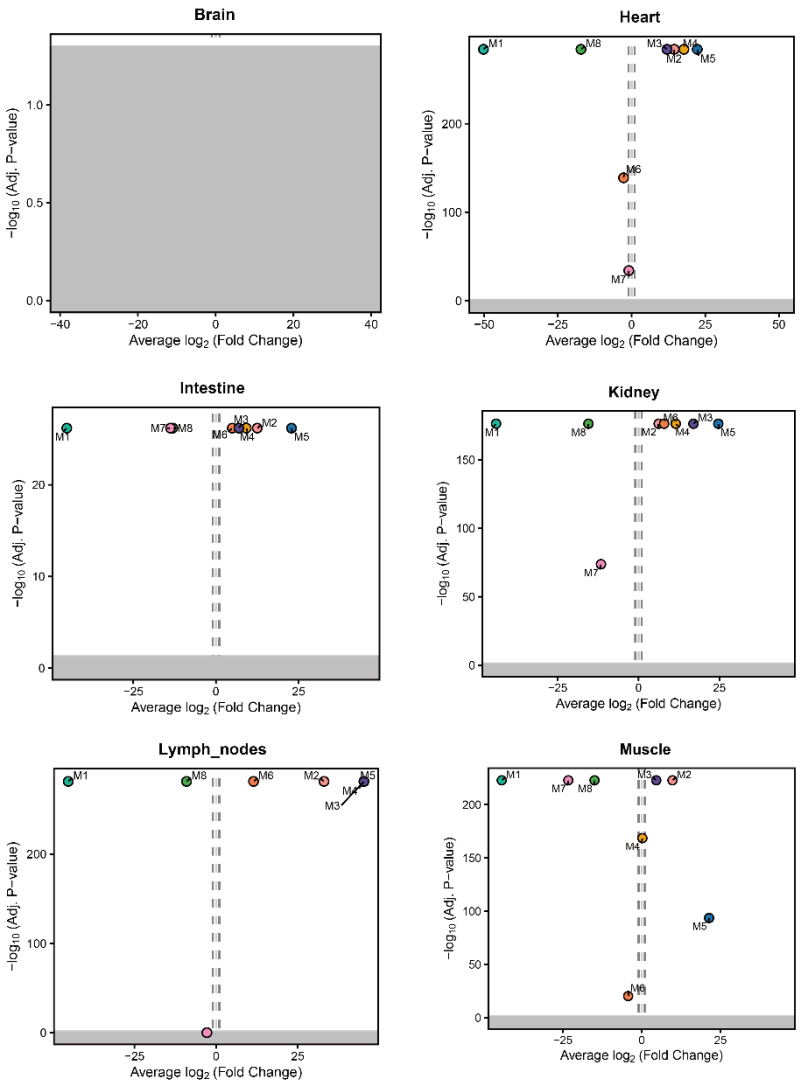

Supplementary Fig. S8 Differential expression analysis of TBP versus LWP modules (cold adaptation).

Gray denotes regions without associated modules. Modules to the left of the dashed line are downregulated, and those to the right are upregulated.

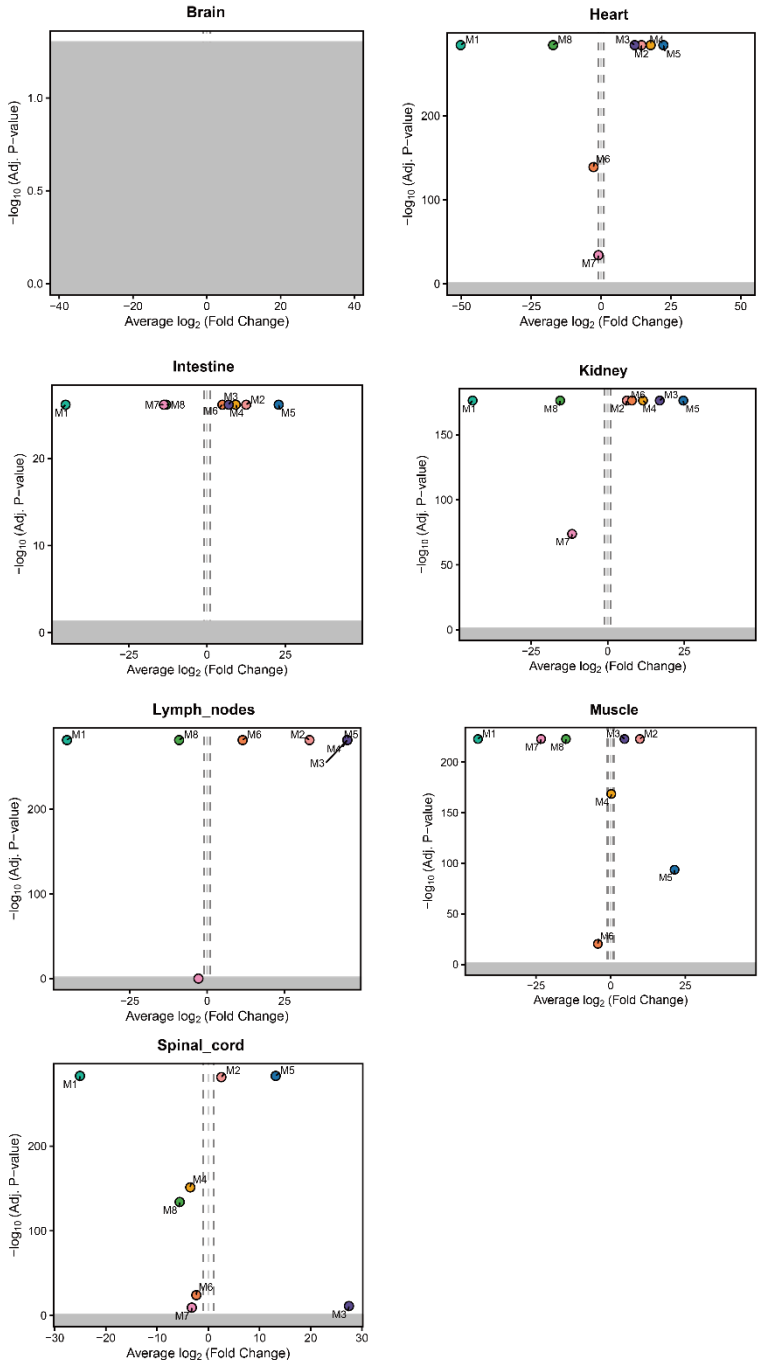

Supplementary Fig. S9 TBP-LWP module differential expression analysis (hypoxic adaptation).

Gray denotes regions without associated modules. Modules to the left of the dashed line are downregulated, and those to the right are upregulated.

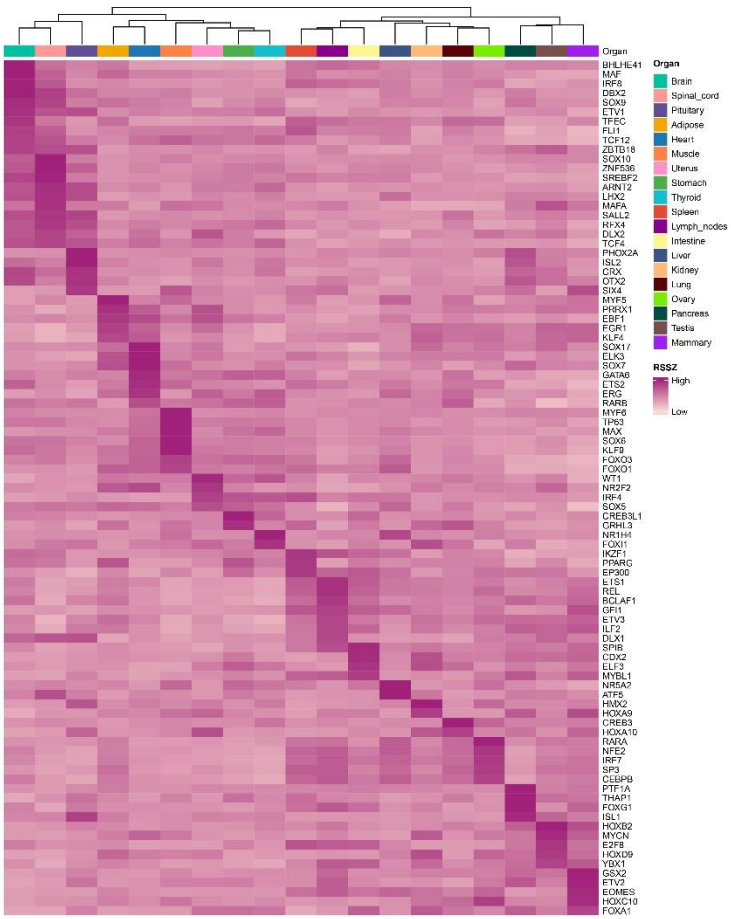

Supplementary Fig. S10 Heatmap of RSSZ values for shared regulators in selected organs of TBP and LWP.

The top-ranked regulator by RSSZ value was labeled for each organ.

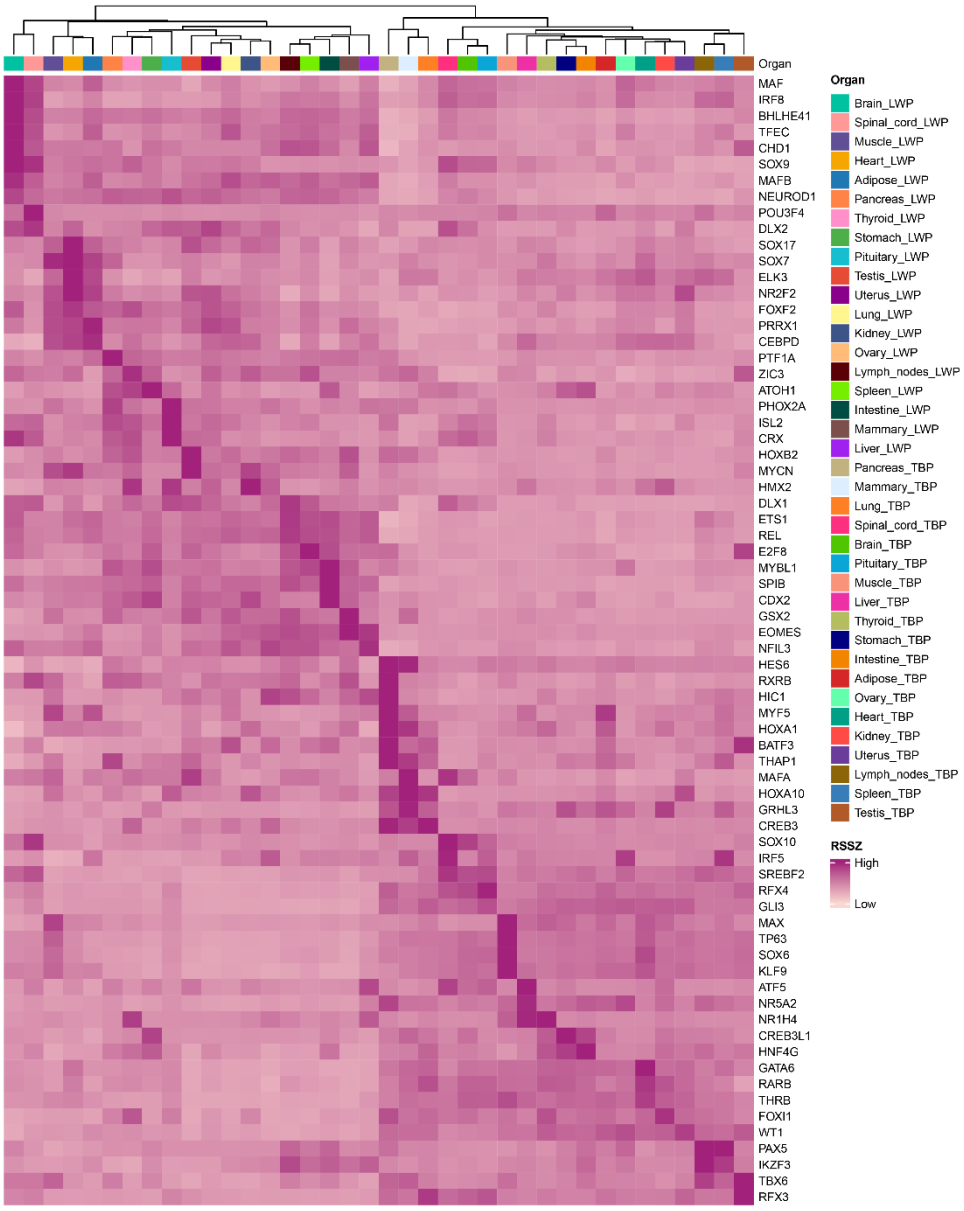

Supplementary Fig. S11 Heatmap of RSSZ values of regulators in shared organs between TBP and LWP, with separate profiling of the two breeds within each matched organ.

The top-ranked regulator by RSSZ value was labeled for each organ.

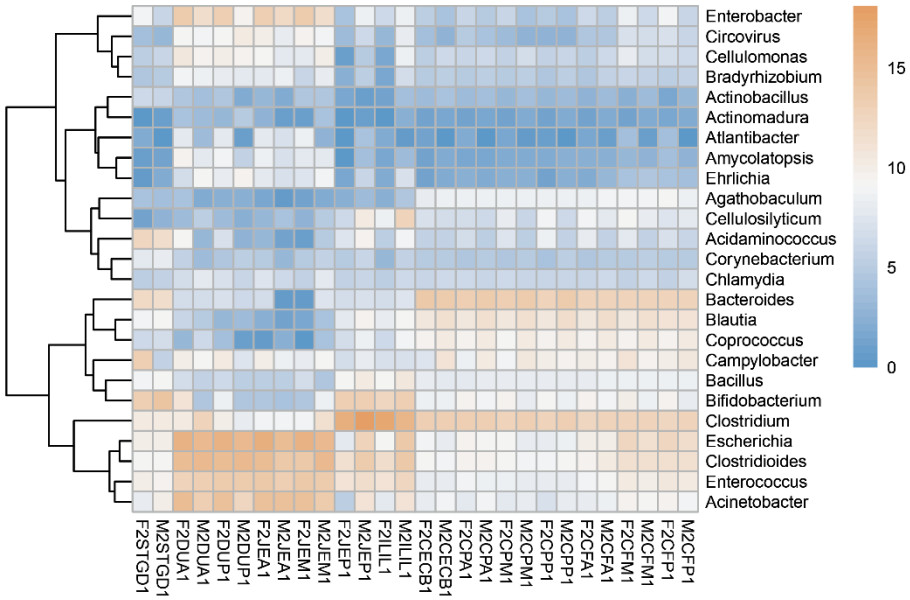

Supplementary Fig. S12 Heatmap showing microbiota abundance in gastrointestinal samples (pre-filtering).

The x-axis shows gastrointestinal samples and the y-axis shows bacterial genera. Increasing blue intensity denotes lower abundance.

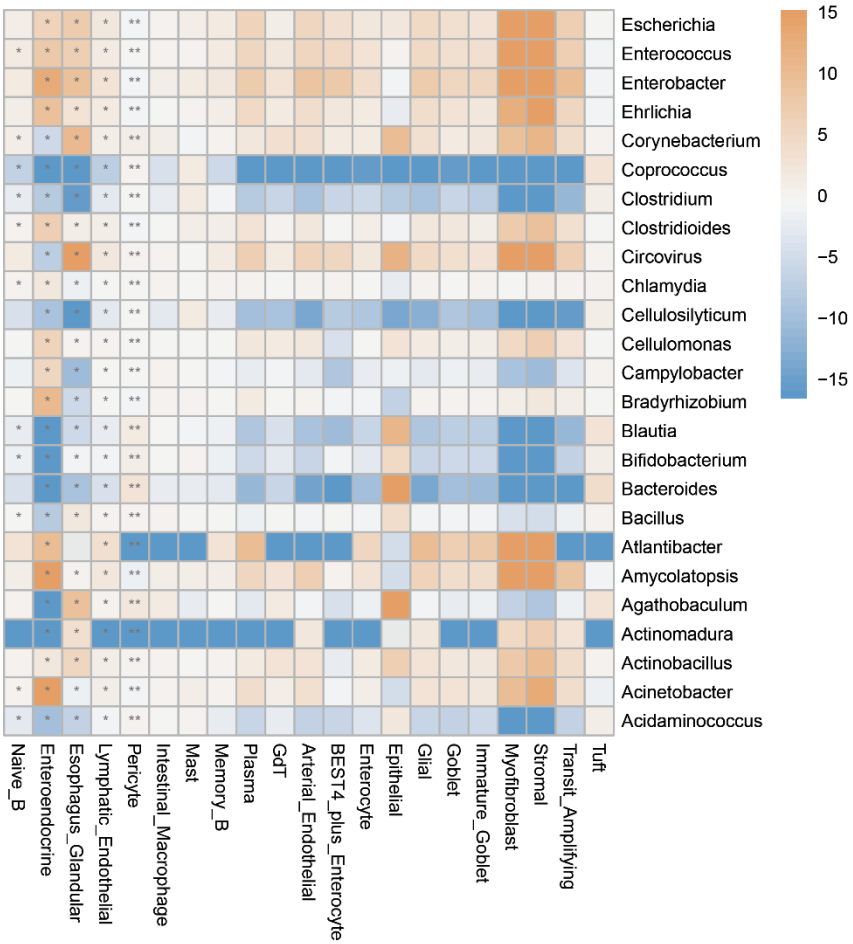

Supplementary Fig. S13 Heatmap illustrating cell type-microbiota associations in the gastrointestinal tract (pre-filtering).

The x-axis shows gastrointestinal cell types and the y-axis shows bacterial genera. Blue denotes negative correlation, and red denotes positive correlation.

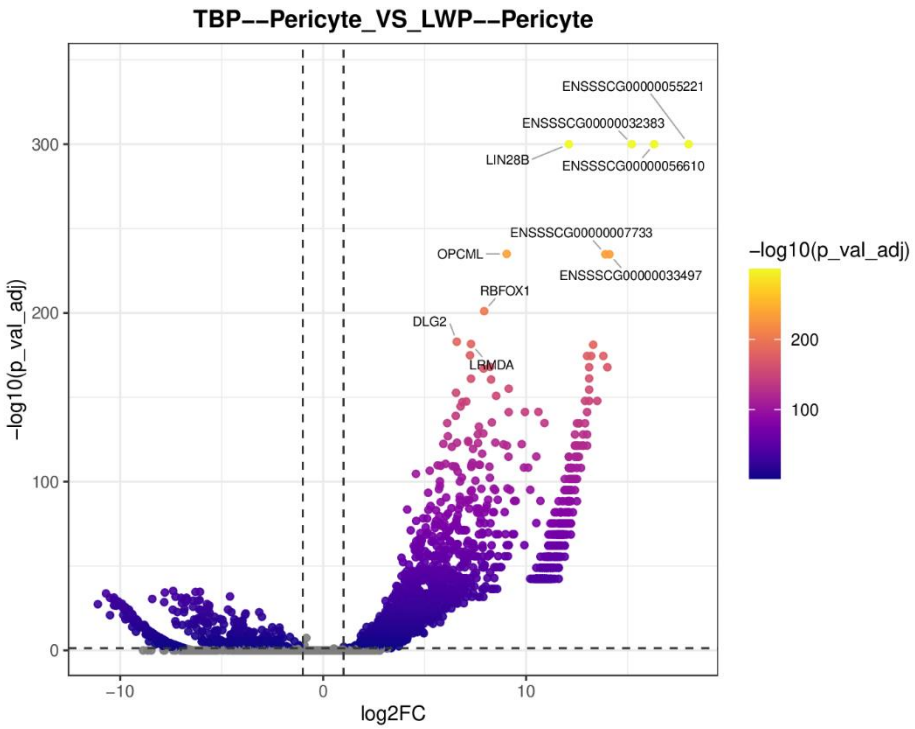

Supplementary Fig. S14 Volcano plot of DEGs in pericytes (TBP vs LWP).

Significant upregulation: avg_$\log_2$FC > 1, adjusted p-value < 0.05; significant downregulation: avg_$\log_2$FC < −1, adjusted p-value < 0.05.

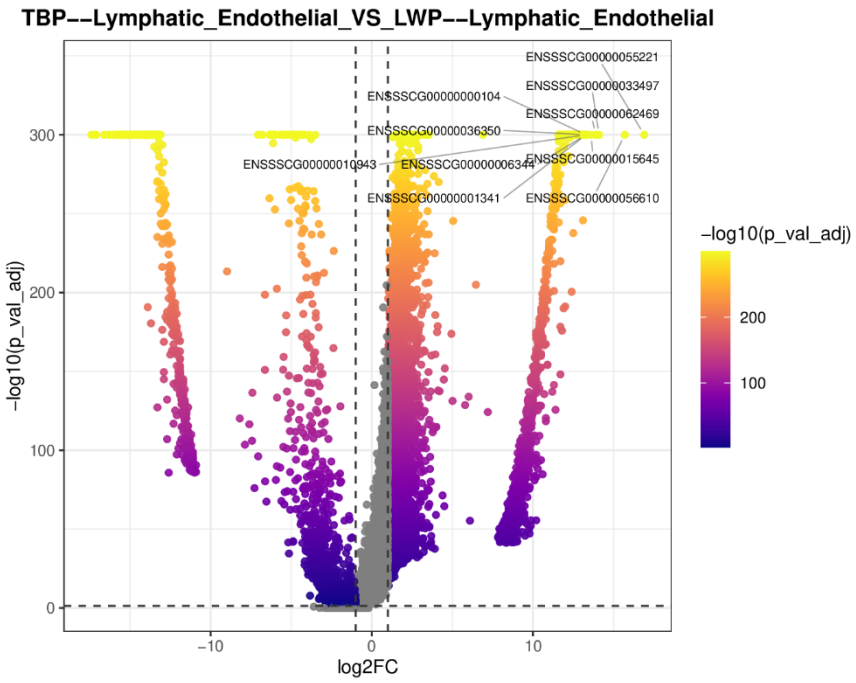

Supplementary Fig. S15 Volcano plot of DEGs in Lymphatic_Endothelial (TBP vs LWP). Significant upregulation: avg_$\log_2$FC > 1, adjusted p-value < 0.05; significant downregulation: avg_$\log_2$FC < −1, adjusted p-value < 0.05.

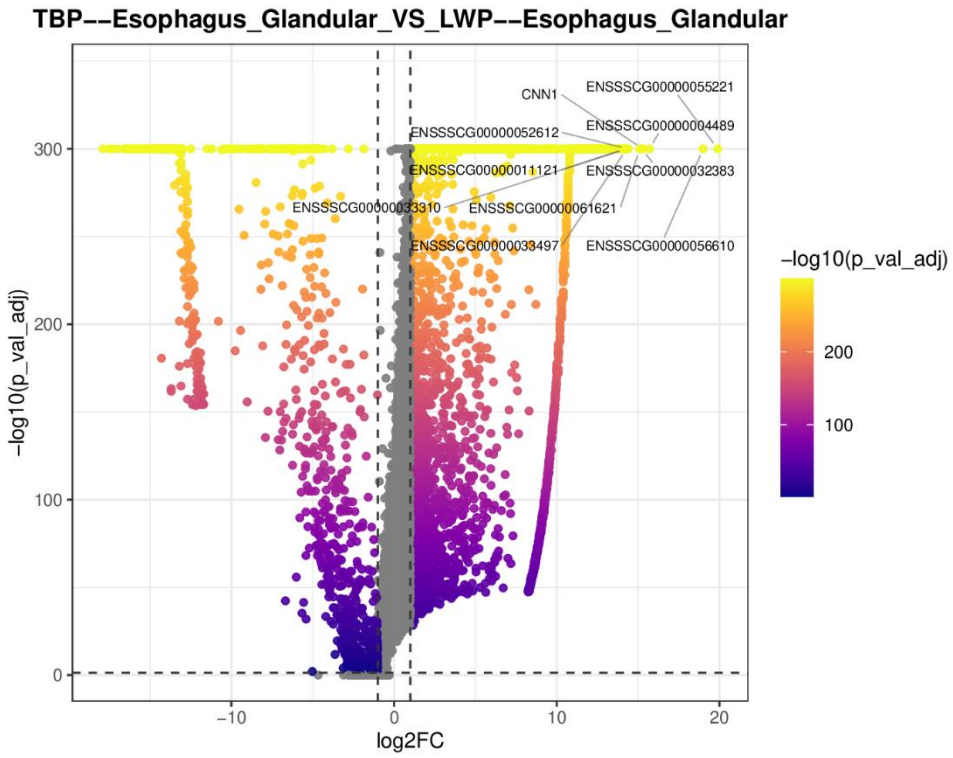

Supplementary Fig. S16 Volcano plot of DEGs in Esophagus_Glandular (TBP vs LWP).
Significant upregulation: avg_$\log_2$FC > 1, adjusted p-value < 0.05; significant downregulation: avg_$\log_2$FC < −1, adjusted p-value < 0.05.

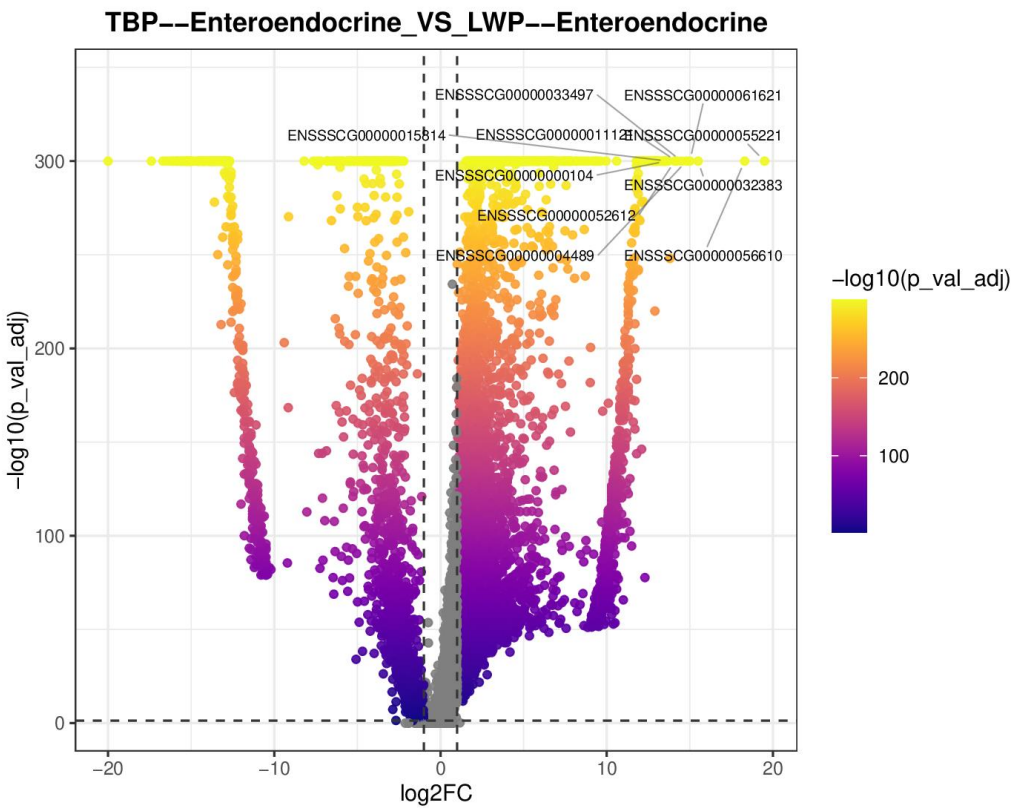

Supplementary Fig. S17 Volcano plot of DEGs in Enteroendocrine (TBP vs LWP).

Significant upregulation: avg_$\log_2$FC > 1, adjusted p-value < 0.05; significant downregulation: avg_$\log_2$FC < −1, adjusted p-value < 0.05.

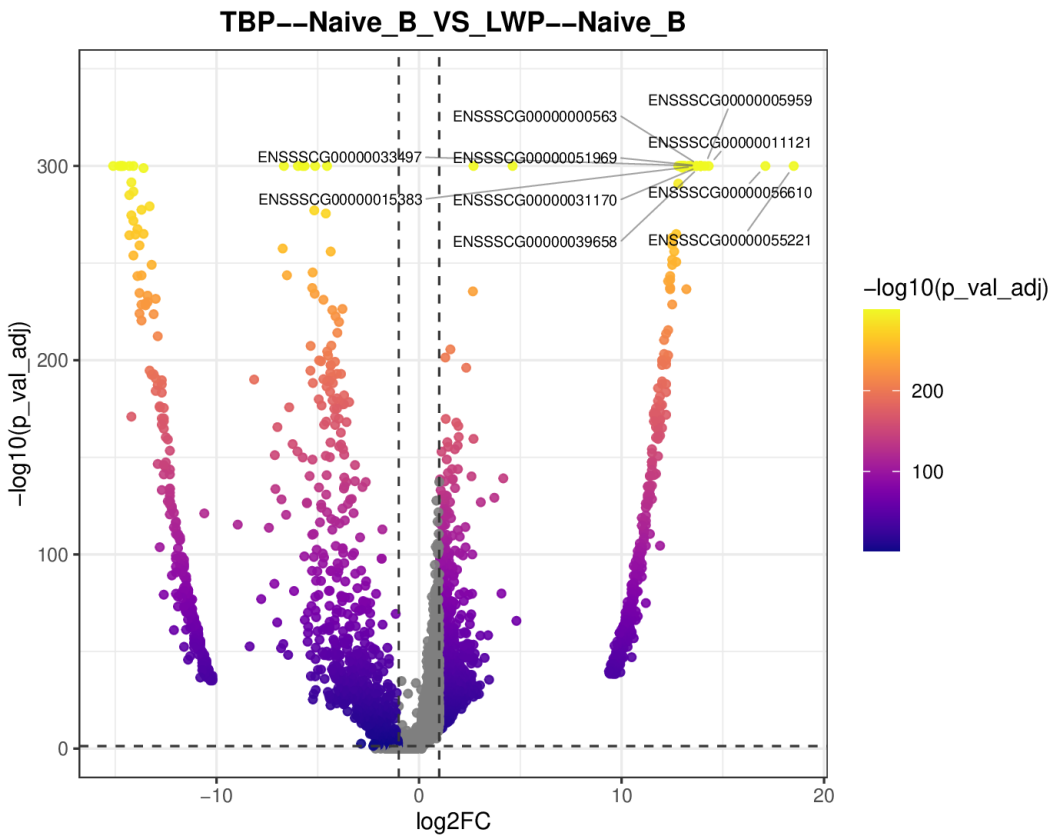

Supplementary Fig. S18 Volcano plot of DEGs in Naive_B (TBP vs LWP).

Significant upregulation: avg_$\log_2$FC > 1, adjusted p-value < 0.05; significant downregulation: avg_$\log_2$FC < −1, adjusted p-value < 0.05.

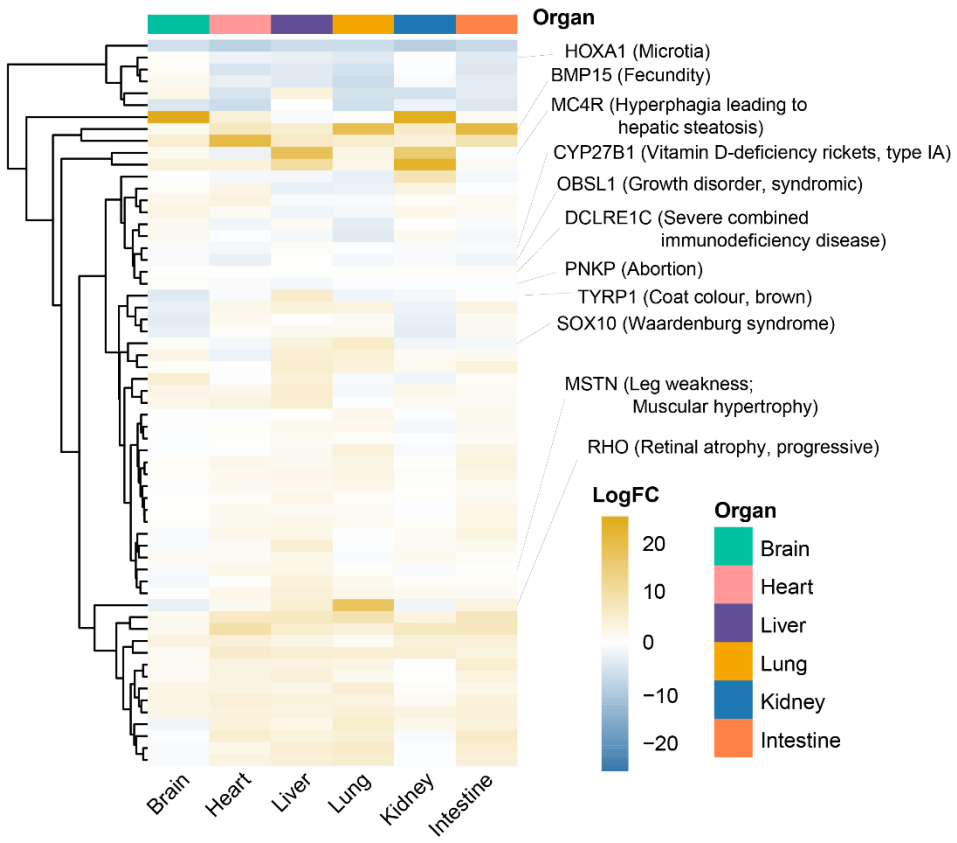

Supplementary Fig. S19 Heatmap of differentially expressed Mendelian disease genes in humans and Tibetan pigs across different organs.

This heatmap displays the LogFC values of 11 Mendelian disease genes. The X-axis represents the different organs (Brain, Heart, Liver, Lung, Kidney, Intestine). The cluster indicated by the arrow in the figure denotes genes associated with Mendelian diseases in both humans and Tibetan pigs.